

Tissue-type plasminogen activator–mediated shedding of astrocytic low-density lipoprotein receptor–related protein increases the permeability of the neurovascular unit

Rohini Polavarapu,¹ Maria Carolina Gongora,¹ Hong Yi,² Sripriya Ranganathan,³ Daniel A. Lawrence,⁴ Dudley Strickland,⁵ and Manuel Yepes¹

¹Department of Neurology and Center for Neurodegenerative Disease, Emory University School of Medicine, Atlanta, GA; ²Microscope Core Center, Emory University, Atlanta, Georgia; ³Center for Vascular and Inflammatory Diseases, University of Maryland School of Medicine, Baltimore; ⁴Department of Internal Medicine, University of Michigan, Ann Arbor; ⁵Departments of Surgery and Physiology, University of Maryland School of Medicine, Baltimore

The low-density lipoprotein receptor–related protein (LRP) is a member of the LDL receptor gene family that binds several ligands, including tissue-type plasminogen activator (tPA). tPA is found in blood, where its primary function is as a thrombolytic enzyme, and in the central nervous system where it mediates events associated with cell death. Cerebral ischemia induces changes in the neurovascular unit (NVU) that result in brain edema. We investigated whether the interaction

between tPA and LRP plays a role in the regulation of the permeability of the NVU during cerebral ischemia. We found that the ischemic insult induces shedding of LRP's ectodomain from perivascular astrocytes into the basement membrane. This event associates with the detachment of astrocytic end-feet processes and the formation of areas of perivascular edema. The shedding of LRP's ectodomain is significantly decreased in tPA deficient (tPA^{-/-}) mice, is increased by

incubation with tPA, and is inhibited by the receptor-associated protein (RAP). Furthermore, treatment with either RAP or anti-LRP IgG results in a faster recovery of motor activity and protection of the integrity of the NVU following middle cerebral artery occlusion (MCAO). Together, these results implicate tPA/LRP interactions as key regulators of the integrity of the NVU. (Blood. 2007;109:3270-3278)

© 2007 by The American Society of Hematology

Introduction

The low-density lipoprotein receptor–related protein (LRP) is a member of the LDL receptor gene family composed of a 515-kDa heavy chain noncovalently bound to an 85-kDa light chain containing a transmembrane and a cytoplasmic domain.¹ LRP mediates the internalization of apoE-enriched lipoprotein particles,² α -2-macroglobulin–protease complexes,³ and several other ligands, including plasminogen activators, proteinase-inhibitor complexes, clotting factors, and the amyloid precursor protein (APP).¹ LRP has also been implicated in cellular signal transduction pathways⁴ and neurotransmission.⁵ Like other signaling receptors such as Notch⁶ and APP,⁷ LRP undergoes a γ -secretase-like–dependent cleavage of its cytoplasmic site with release of its intramembranous domain.⁸ This process is preceded by shedding of the receptor's ectodomain which may increase substrate availability for the enzymes that are required for the cleavage of the intramembranous or cytosolic sites.^{8,9}

Tissue-type plasminogen activator (tPA) is a ligand for LRP,^{10,11} on binding to LRP induces a transient tyrosine phosphorylation of its cytoplasmic domain, and induces increased synthesis of MMP-9.^{12,13} Animal studies have demonstrated that following the onset of cerebral ischemia there is an increase in endogenous tPA activity within the ischemic tissue,^{14–16} and that either genetic deficiency of tPA^{14,17} or its inhibition with neuroserpin^{15,18} are associated with neuronal survival and decrease in the volume of the ischemic lesion.

The neurovascular unit (NVU) is a dynamic structure consisting of endothelial cells, the basal lamina, astrocytic end-feet processes, pericytes, and neurons.^{19,20} One of the functions of the NVU is to form a barrier, known as the blood-brain barrier (BBB), that regulates the entry of selected molecules from the blood into the central nervous system (CNS).^{21,22} During cerebral ischemia the permeability of the NVU increases, resulting in the development of cerebral edema,^{23,24} which is a major cause of death among patients with acute stroke. It has been demonstrated that the interaction of tPA with LRP plays a role in the regulation of cerebrovascular tone²⁵ and permeability of the NVU¹⁶ under nonischemic conditions.

In the studies presented here, we demonstrate that during cerebral ischemia tPA induces cleavage of LRP with shedding of LRP's ectodomain from the surface of astrocytic end-feet processes into the basement membrane. This tPA-mediated cleavage of LRP is associated with astrocytic swelling, detachment of astrocytic end-feet processes from the basement membrane, and increase in the permeability of the NVU. Together, our results demonstrate that the augmentation in the permeability of the NVU following the onset of the ischemic insult is an event mediated by the interaction between tPA and LRP. In addition, preventing the binding of tPA to LRP by using the receptor antagonist RAP results in decrease of cerebral ischemia-induced shedding of LRP's ectodomain, preservation of the structure and permeability of the NVU, and faster recovery in motor activity following middle cerebral artery occlusion (MCAO).

Submitted August 21, 2006; accepted December 6, 2006. Prepublished online as *Blood* First Edition Paper, December 14, 2006; DOI 10.1182/blood-2006-08-043125.

The publication costs of this article were defrayed in part by page charge

payment. Therefore, and solely to indicate this fact, this article is hereby marked "advertisement" in accordance with 18 USC section 1734.

© 2007 by The American Society of Hematology

Materials and methods

Antibodies

The 11H4 mouse monoclonal antibody, prepared against the 13 amino acids representing the C-terminus of LRP,²⁶ was purified from cell lines purchased from the American Type Culture Collection (ATCC; Manassas, VA). R2629 is a rabbit polyclonal antibody that was prepared by immunizing rabbits with purified human LRP as described elsewhere.^{27,28} In addition, this study also used a goat anti-LRP that was prepared by immunizing a goat with purified human LRP.¹⁶

Animal models

Mice and rats were anesthetized with 4% chloral hydrate. The rectal and masseter muscle temperatures were controlled at 37°C with a homeothermic blanket. Cerebral perfusion (CP) in the distribution of the middle cerebral artery was monitored throughout the surgical procedure with a laser Doppler scan (Perimed, North Royalton, OH), and only animals with a greater than 80% decrease in CP were included in this study. The middle cerebral artery was exposed and occluded in mice with a 10-0 suture as described.^{16,17} Murine strains were tPA-deficient (tPA^{-/-}) mice and their C57BL/6J wild-type (WT) controls. Immediately after MCAO, a subgroup of mice were placed on a stereotaxic frame and intracortically injected with 2 μ L of either murine tPA (1 μ M; Molecular Innovations, Royal Oak, MI) or PBS at bregma (-1 mm), mediolateral (3 mm), and dorsoventral (3 mm)²⁹ followed by the intravenous injection of 2% Evans blue dye for the experiments of quantification of vascular permeability. A subset of mice was injected into the third ventricle immediately after MCAO with 5 μ L of either RAP (9 μ M), PBS, or purified goat anti-LRP antibodies (85 μ g/mL) as described elsewhere.³⁰ The injections were performed over 5 minutes, and the infusion rate was controlled by a microsyringe pump controller (World Precision Instruments, Sarasota, FL) attached to a syringe holder (World Precision Instruments). After the end of the infusion the needle was left in place for 5 minutes to avoid reflow. To study the distribution of RAP in the ischemic tissue following its intraventricular administration, purified RAP was labeled with Alexa Fluor 546 dye using the Alexa Fluor labeling kit (Molecular Probes, Invitrogen, Leiden, The Netherlands). Mice underwent MCAO followed by treatment with fluorescently labeled RAP. Six hours later brains were harvested, cut onto 10- μ m sections, and stained for DAPI. Fluorescently labeled RAP was detected in the ischemic tissue in each one of the 3 areas of interest (AOIs; data not shown). In rats the middle cerebral artery was exposed in Sprague-Dawley males weighing 350 to 400 g and cauterized with a bipolar coagulator as described elsewhere.^{15,31} All procedures were approved by the Emory University Institutional Animal Care and Use Committee.

Magnetic resonance imaging (MRI)

Immediately after MCAO animals were placed into a stereotaxic headset and on a cradle with a built-in surface coil (2.3-cm ID) for brain imaging and a neck coil for cerebral blood flow (CBF) labeling. Diffusion- and perfusion-weighted images were acquired at 30, 60, 90, 120, and 180 minutes after ischemia. The average apparent diffusion coefficient (ADC_{ave}) of water was obtained by averaging 3 ADC maps acquired separately with diffusion-sensitive gradients applied along the x, y, or z direction. Single-shot, spin-echo, echo-planar images (EPIs) were acquired with matrix = 64 \times 64, FOV = 2.56 \times 2.56 cm², 7 1.5-mm slices, TR = 2 s (90° flip angle), TE = 28 ms, b = 0 and 1200 s/mm², Δ = 15 ms, γ = 3.5 ms, and 16 averages. Quantitative CBF was measured using the continuous arterial spin-labeling technique with single-shot, gradient-echo EPI. Anatomical T₂-weighted images were acquired at 3 hours after ischemia using the fast spin-echo (RARE) pulse sequence with TR = 2 s (90° flip angle), effective TE = 55 and 102 ms, matrix = 128 \times 128, 8 echo trains, 16 averages.

Immunohistochemistry and definition of areas of interest (AOIs)

Twenty frozen brain sections 10 μ m each were obtained 24 hours after MCAO in mice or 180 minutes after MCAO and MRI in rats and stained with either a polyclonal antibody (R2629) that detects the intracellular and extracellular domains of LRP (1:1000 dilution) or a monoclonal antibody (11H4) that detects only the intracellular domain of LRP (1:500 dilution).²⁶ Sections were costained with either a polyclonal rabbit anti-human von Willebrand factor antibody (1:200 dilution; Dako, Carpinteria, CA) or an anti-mouse CD31 (PECAM-1) monoclonal antibody (1:100 dilution; BD Biosciences, San Jose, CA). Each coronal section was then divided into 16 square areas (150 mm² each one) that involved the necrotic core and the area of ischemic penumbra and comparable areas in the nonischemic hemisphere. Two areas of interest (AOIs) were chosen in the boundaries between the ischemic penumbra and necrotic core (AOI-1 and AOI-3), whereas a third zone was located in the necrotic core (AOI-2). To determine the number of LRP-positive vascular structures, images were digitized in a Zeiss (Jena, Germany) Axioplan 2 microscope (20-fold objective) with a Zeiss AxioCam and imported into AxioVision. Images were then viewed at 150% of the original \times 20 images with Image MetaMorph software (Molecular Devices, Sunnydale, CA). The number of LRP-positive vascular structures counted in the described AOI was organized in a 2-way comparison table for the ischemic and the nonischemic hemispheres. Four animals were included in each experimental group.

Immunogold electron microscopy

Six mice were deeply anesthetized after MCAO and perfused transcardially with a phosphate-buffered solution as described elsewhere,³² followed by incubation with the R2629 and 11H4 anti-LRP antibodies (1:1000 dilution). Control sections were treated identically, except they received no primary antibody. LRP immunostaining was amplified by incubating sections in avidin-biotin-HRP (Vector Laboratories, Burlingame, CA). After resin was polymerized, the AOI and the corresponding zones in the contralateral nonischemic tissue were dissected out and treated as described elsewhere.³²

Studies of motor activity and evaluation of the permeability of the NVU

Six hours before MCAO and 6, 24, and 48 hours thereafter animals were placed in individual acrylic chambers for 2 hours, and horizontal and vertical motor activities were recorded with an Omnitech Digiscan Activity Monitor (Omnitech Instruments, Columbus, OH) as described elsewhere.³³ The number and extent of horizontal and vertical movements were determined by breaks in photo beams and converted into locomotor activity counts. Results for each time point were compared with the baseline evaluation obtained 6 hours before the surgical procedure. Immediately after the last motor evaluation, brains were removed and homogenized, and Evans blue dye extravasation was quantified as described elsewhere.¹⁶ Six animals were included in each experimental group. Statistical analysis was performed with the Student *t* test.

Western blot analysis

Astrocytes were cultured from 1-day-old wild-type and tPA^{-/-} C57BL/6J mice as described elsewhere.³⁴ Cultures were treated 10 days later with serum-free media for 24 hours, washed with PBS 3 times, and then incubated under oxygen-glucose deprivation (OGD) conditions for 6 hours in an anaerobic chamber (Billups-Rothenberg, Del Mar, CA). A less than 5% oxygen concentration was confirmed with an oximeter before starting the experiment. In preliminary studies we used a colorimetric assay to quantify the release of lactate dehydrogenase (LDH) in the media of cultured astrocytes (Oxford Biomedical Research, Oxford, MI). We found that exposure to OGD conditions for 6 hours results in less than 10% release of LDH compared with cultures treated with the cell-lysing reagent provided by the manufacturer (data not shown). As a control, a similar group of cells was kept under normoxic conditions. A subset of astrocytes cultured from wild-type mice were incubated with 2 mL of either PBS or murine tPA (1 μ M; Molecular Innovations) or the combination of murine

tPA (1 μ M) and RAP (10 μ M). A third group of astrocytes from wild-type mice were exposed to OGD conditions with and without RAP (10 μ M). After 6 hours of exposure to either OGD or normoxic conditions, conditioned media was collected and centrifuged at 800g. The collected supernatants were centrifuged again at 16 000g for 15 minutes, and the supernatant was removed and concentrated using centricon 30 (Millipore, Bedford, MA). The concentrated samples were incubated with 10 μ L strata clean resin (Stratagene; La Jolla, CA) for 30 minutes and centrifuged. The sample was boiled with 25 μ L of 2 \times nonreducing SDS gel sample buffer and separated on a 4% to 12% acrylamide gel before transfer to a nitrocellulose membrane. The heavy chain of LRP was detected using an anti-LRP affinity-purified goat IgG. Twelve micrograms of cell lysates from each one of the experimental conditions was processed under similar conditions and probed with an anti-LRP goat IgG. For the loading control, membranes were probed with an anti- β -actin antibody (Sigma, St Louis, MO). Each observation was repeated 4 times. The mean density of the band in the media was quantified with the NIH Image Analyzer System, and results were presented as a mean density of the band. Statistical analysis was performed with the Student *t* test.

Results

Relationship between the development of cerebral edema and LRP immunostaining in the ischemic brain

To study the relation between the formation of the areas of necrotic core, ischemic penumbra and developing cerebral edema, and changes in the pattern of LRP immunostaining, rats underwent continuous monitoring of cerebral blood flow (CBF), apparent diffusion coefficient (ADC) of water (detects irreversibly injured brain tissue), and anatomical T_2 -weighted images (sensitive to the presence of tissue changes associated with evolving edema)³⁵ 180 minutes after MCAO, followed by immunohistochemical analysis of brain sections with the R2629 and 11H4 anti-LRP antibodies.

We found that 3 hours after the onset of the ischemic insult there is a well-defined area of decreased CBF (pointed by white arrows in Figure 1A) and irreversibly injured brain tissue (depicted by white arrows in Figure 1B). Likewise, T_2 -weighted images revealed the presence of an area of evolving cerebral edema (hyperintense signal marked by the white arrows in Figure 1C). Staining with both R2629 and 11H4 antibodies showed absence of LRP immunoreactivity in the necrotic core. In contrast, staining with the R2629 antibody detected the presence of LRP immunostaining around blood vessels in the area of evolving cerebral edema (Figure 1D-F). This pattern of immunostaining was not observed when the contralateral nonischemic hemisphere was stained with the same antibody (Figure 1G-I). Staining with the 11H4 antibody did not detect the presence of LRP around the blood vessels in the area with developing cerebral edema (Figure 1J-L). Instead, it detected the intracellular domain of LRP in the ipsilateral (Figure 1K-L) and contralateral (Figure 1N-O) hemispheres.

Quantification of LRP-positive vascular structures in the murine brain

To study the effect of cerebral ischemia on the pattern of LRP immunostaining in the murine brain and to quantify the presence of LRP-positive vascular structures in the area with developing cerebral edema, we performed immunohistochemical staining of brain sections of wild-type mice 24 hours after MCAO with the 11H4 and R2629 antibodies. As observed in the rat brain, staining with the R2629 and 11H4 antibodies demonstrated absence of LRP staining in the necrotic core (Figure 2A-B). In contrast, the R2629 antibody detected LRP immunoreactivity around blood vessels in

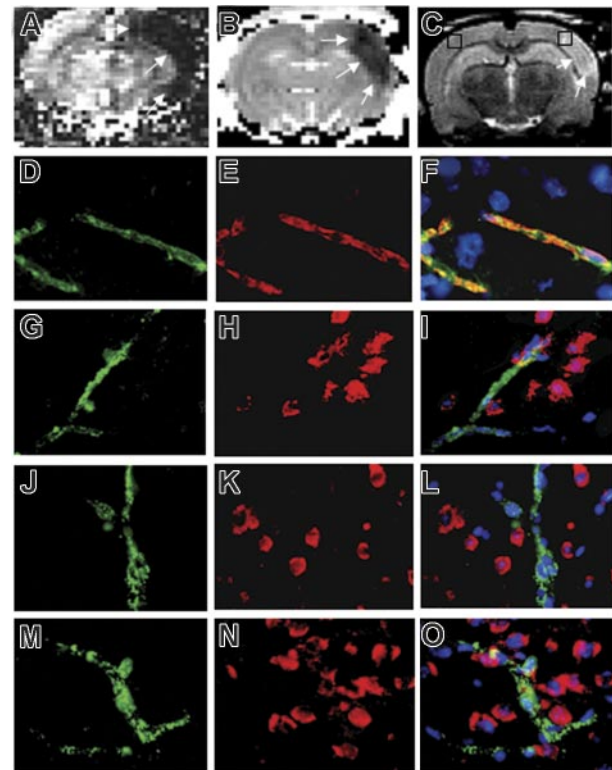


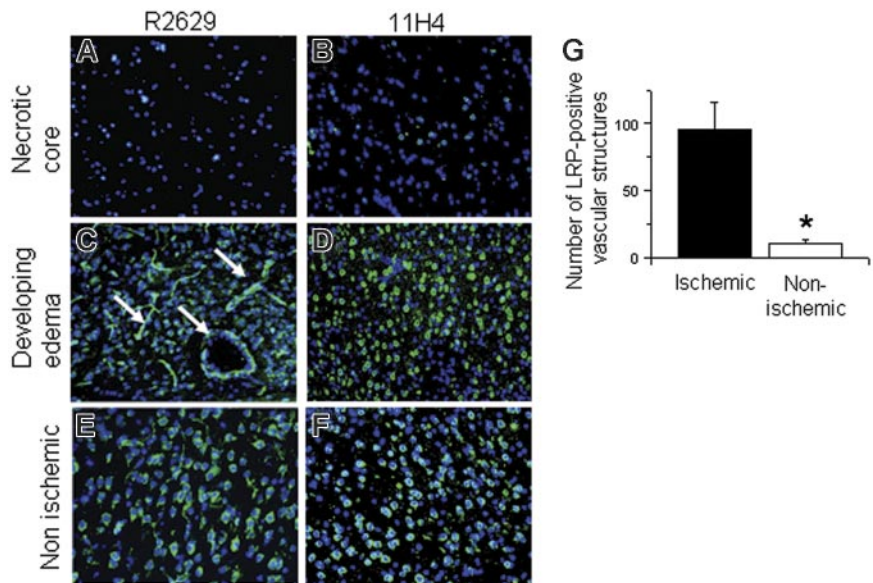
Figure 1. Immunohistochemical staining of LRP in the ischemic brain 3 hours after middle cerebral artery occlusion. Animals were subjected to MCAO followed by continuous MRI monitoring of cerebral blood flow (CBF), apparent diffusion coefficient (ADC) of water, and tissue changes associated with cerebral edema (T_2 -weighted images), followed by immunohistochemical analysis of LRP expression 180 minutes after the onset of the ischemic insult. (A-B) Changes in CBF (A) and ADC of water (B) 30 minutes after MCAO. Arrows in panel A depict the area of the brain with a greater than 80% decrease in CBF (dark zone). Arrows in panel B denote the area of irreversibly injured brain (dark area). (C) T_2 -weighted image of the same brain of panels A and B. Arrows depict the edge of the ischemic tissue with evolving cerebral edema (hyperintense signal). The black squares represent the areas of the brain where the immunohistochemical staining for LRP expression was performed. (D-I) Immunohistochemical staining with an antibody against CD31 (PECAM-1) (D,G) and the R2629 LRP antibody (E,H) in the area corresponding to the black squares in the ischemic (D-F) and nonischemic (G-I) hemispheres. Panels F and I correspond to merged images. (J-O) Immunohistochemical staining with an antibody against von Willebrand factor (J,M) and the 11H4 LRP antibody (K,N) in the area corresponding to the black squares depicted in panel C in the ischemic (J-L) and nonischemic (M-O) hemispheres. Panels L and O correspond to merged images. Images were visualized using a Leica DMRBE microscope (Leica, Houston, TX) equipped with a 100 \times /1.30 numerical aperture (NA) oil objective lens and a Leica DC 500 camera. Images were processed using software provided by the camera manufacturer.

the area with developing cerebral edema (Figure 2C, arrows) that was not observed when the same area was stained with the 11H4 antibody (Figure 2D). Finally, neither the R2629 nor the 11H4 antibodies detected the presence of LRP immunoreactivity around blood vessels in the contralateral nonischemic hemisphere (Figure 2E-F). To further characterize these results we quantified the number of LRP-positive vascular structures in each one of the AOIs in the ischemic and nonischemic hemispheres as described in "Materials and methods." We found that the number of these structures decreased from 96 ± 20 in the ischemic tissue to 10 ± 3 in the contralateral, nonischemic hemisphere (Figure 2G; $n = 6$; $*P < .05$).

Effect of cerebral ischemia on LRP in the NVU

To further study the effect of cerebral ischemia on LRP in the NVU in the area with developing cerebral edema, we performed electron

Figure 2. Development of LRP-positive vascular structures in the murine brain 24 hours after middle cerebral artery occlusion. Wild-type mice were subjected to MCAO and killed 24 hours later. Tissue sections were prepared from the necrotic core (A-B), area of developing edema (C-D), and a corresponding area in the healthy, nonischemic contralateral hemisphere (E-F) and stained with either the R2629 (A,C,E) or the 11H4 antibody (B,D,F). Green is LRP staining and blue is DAPI. Arrows depict examples of LRP-positive vascular structures. (G) Number of LRP-positive vascular structures in the 3 areas of interest in the ischemic and nonischemic hemispheres 24 hours after the onset of cerebral ischemia. Error bars describe standard error of the mean; $n = 6$; $*P < .05$. Magnification, $\times 40$ (A-F). Images were acquired as in Figure 1, except that a $40\times/0.70$ NA objective was used.



microscopy analysis of brain sections of wild-type mice 6 hours after MCAO. Staining with the R2629 antibody (Figure 3A,C,E) detected the presence of LRP's ectodomain in the basement membrane of the ischemic NVU (Figure 3A,C) that was not seen in the contralateral nonischemic hemisphere (Figure 3E) or when the ischemic sections were stained with the 11H4 antibody (Figure 3B,D,F). Instead, the 11H4 antibody showed the presence of LRP in the intracellular compartment of perivascular astrocytes (Figure

3B,D,F). Higher magnification demonstrated that those areas of the basement membrane where the ectodomain of LRP was detected with the R2629 antibody corresponded to zones of detachment of astrocytic end-feet from the underlying glia limitans with development of areas of perivascular edema (Figure 3C, asterisks). In contrast, staining with the 11H4 antibody did not detect the presence of LRP immunoreactivity in the areas of the basement membrane with detachment of astrocytic end-feet processes (Figure 3D, dashed arrows) and development of perivascular edema (Figure 3D, asterisks).

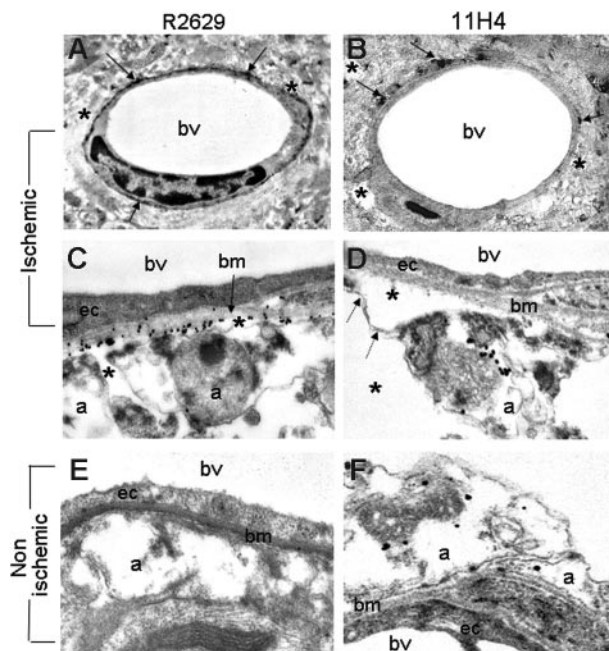


Figure 3. Effect of cerebral ischemia on LRP in the neurovascular unit. Electron microscopy analysis of LRP expression in the NVU in the ischemic (A-D) and corresponding nonischemic (E-F) hemispheres 6 hours after MCAO. Brains were stained with either the R2629 (A,C,E) or the 11H4 (B,D,F) antibodies. Arrows in panel A depict the presence of LRP-positive areas surrounding the blood vessel. Arrows in panel B point to LRP-positive perivascular astrocytes. Asterisks in panels A to D show areas where the perivascular astrocyte has detached from the basement membrane with development of early perivascular edema. Dashed arrows in panel D depict areas of astrocytic detachment of the glia limitans. Bv indicates blood vessel; bm, basement membrane; a, perivascular astrocyte; ec, endothelial cell. Magnification, $\times 5000$ (A-B) and $\times 30\,000$ (C-F). Images were visualized using a Hitachi H-7500 electron microscope (Hitachi, Tokyo, Japan).

Effect of RAP and anti-LRP antibodies on the shedding of LRP's ectodomain, motor recovery, and blood-brain barrier (BBB) permeability following MCAO

To characterize the relation between cerebral ischemia-induced shedding of LRP's ectodomain, recovery of motor function, and increase in the permeability of the BBB, we quantified the number of LRP-positive vascular structures, changes in mean locomotor activity, and Evans blue dye extravasation in wild-type mice following MCAO and treatment with either PBS, the receptor-associated protein (RAP), or purified goat anti-LRP antibodies. The presence of LRP-positive vascular structures was quantified in the 3 AOIs 24 hours after MCAO as described in "Materials and methods." Locomotor activity was evaluated 6 hours before MCAO and 6, 24, and 48 hours thereafter followed by analysis of BBB permeability by quantification of Evans blue dye extravasation in the same cohort of animals. We found that treatment with either RAP or anti-LRP antibodies resulted in a decrease in the number of LRP-positive vascular structures from 117 ± 22 in PBS-treated animals to 55 ± 17 in RAP-treated mice and 68 ± 22 in animals that received anti-LRP treatment (Figure 4A; $n = 6$; $*P < .05$), as well as in a faster recovery of motor activity (Figure 4B) and in a $70.7\% \pm 17\%$ (RAP) and $52\% \pm 18\%$ (anti-LRP treatment) reduction in Evans Blue dye extravasation 48 hours after MCAO ($n = 6$, $P < .05$; Figure 4C).

tPA increases the permeability of the NVU during cerebral ischemia

To study the role of endogenous tPA activity on the permeability of the NVU and recovery of motor function following MCAO,

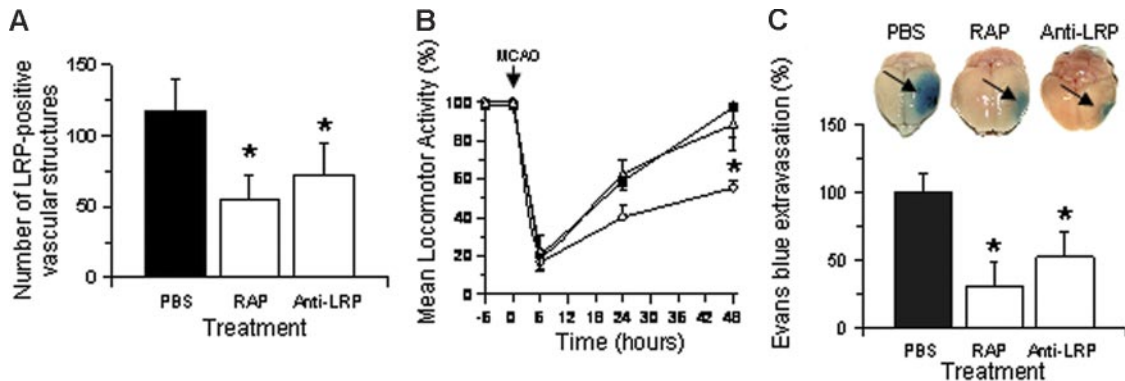


Figure 4. Effect of RAP or anti-LRP antibodies on the shedding of LRP's ectodomain, locomotor activity, and cerebral edema following MCAO. (A) Number of LRP-positive vascular structures in the 3 areas of interest in the ischemic hemisphere of wild-type animals 24 hours after MCAO and treatment with either PBS, the receptor-associated protein (RAP), or goat anti-LRP IgG. Error bars describe standard error of the mean; $n = 6$; $*P < .05$ relative to the PBS-treated group. (B) Mean locomotor activity at 6, 24, and 48 hours after MCAO and the intraventricular administration of either PBS (○), RAP (■), or goat anti-LRP IgG (△). Error bars describe standard error of the mean; $n = 6$; $*P < .05$ when RAP- and LRP-treated animals are compared with PBS-treated mice. (C) Evans blue dye extravasation in the same group of animals of panel B, 48 hours after MCAO. Error bars describe standard error of the mean; $n = 6$; $*P < .05$ relative to PBS-injected brains. The pictures correspond to one representative brain in each experimental group. The blue staining is apparent in areas with increase in blood-brain barrier permeability (arrows).

wild-type and $tPA^{-/-}$ mice underwent MCAO and the intracerebral injection into the ischemic tissue of either PBS or murine tPA. Locomotor activity and BBB permeability were studied in the same cohort of animals as described. We found that, compared with wild-type animals, $tPA^{-/-}$ mice experienced a faster recovery in locomotor activity 24 and 48 hours after MCAO (Figure 5A) and a

87.72% \pm 7.72% reduction in Evans blue dye extravasation 48 hours after the onset of the ischemic insult ($n = 6$; $P < .05$; Figure 5B). In addition, the intracerebral injection of murine tPA into $tPA^{-/-}$ mice after MCAO resulted in a recovery of motor activity (Figure 5A, ▲) and Evans blue dye extravasation (Figure 5B) indistinguishable from that observed in wild-type mice.

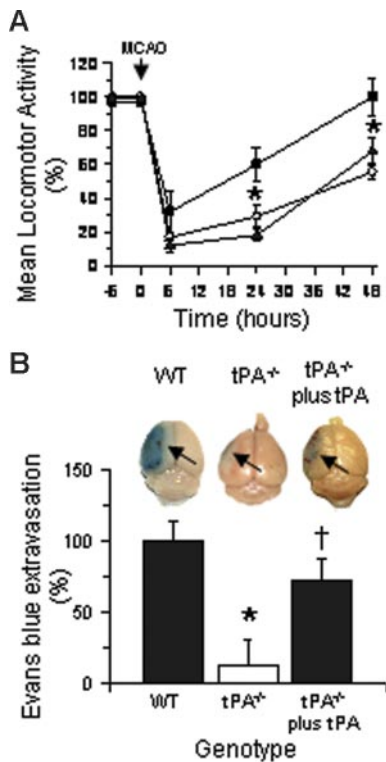


Figure 5. Effect of tPA on locomotor activity and cerebral edema following MCAO. (A) Mean locomotor activity at 6, 24, and 48 hours after MCAO in wild-type (○) or $tPA^{-/-}$ mice (■ and ▲); $tPA^{-/-}$ mice treated with murine tPA immediately after MCAO (▲). Error bars describe standard error of the mean; $n = 6$; $*P < .05$ when $tPA^{-/-}$ mice are compared with wild-type mice or with $tPA^{-/-}$ animals treated with tPA. (B) Evans blue dye extravasation in the same group of animals as panel A 48 hours after MCAO. Error bars describe standard error of the mean. $*P < .01$ when $tPA^{-/-}$ mice are compared with wild-type animals; $\dagger P < .05$ when $tPA^{-/-}$ mice treated with recombinant tPA are compared with untreated $tPA^{-/-}$ mice. The pictures correspond to one representative brain in each experimental group. The blue staining is apparent in areas with increase in blood-brain barrier permeability (arrows).

Endogenous TPA mediates cerebral ischemia-induced shedding of astrocytic LRP's ectodomain

To study the relation between endogenous tPA activity and shedding of LRP's ectodomain during cerebral ischemia, $tPA^{-/-}$ mice underwent MCAO followed by the intracerebral administration of either PBS or recombinant murine tPA. Animals were killed 24 hours later, and immunohistochemical analysis of LRP was performed using the R2629 antibody. The number of LRP-positive vascular structures was determined in the AOIs in the ischemic hemisphere as described in "Materials and methods." We found that the number of LRP-positive blood vessels decreased from 120 ± 32 in wild-type mice to 18 ± 9 in $tPA^{-/-}$ mice and increased to 79 ± 40 in $tPA^{-/-}$ mice treated with murine tPA (Figure 6A; $n = 6$; $*P < .05$). To further characterize these findings we performed electron microscopy analysis with the R2629 antibody in animals subjected to similar experimental conditions. We found that genetic deficiency of tPA resulted in preservation of the structure of the NVU during cerebral ischemia with development of only a few areas of perivascular edema (Figure 6Bi,iii, asterisks). This was accompanied by a minimal shedding of LRP's ectodomain and significant preservation of the astrocytic end-feet processes-basement membrane interaction (Figure 6Bii). In contrast, treatment with recombinant tPA resulted in a significant increase in both the presence of LRP's ectodomain in the basement membrane (Figure 6Bii, arrows) and the development of areas of perivascular edema (Figure 6Bii,iv, asterisks).

TPA induces the shedding of LRP's ectodomain from astrocytes exposed to oxygen-glucose deprivation (OGD) conditions

To further test the hypothesis that tPA mediates the shedding of LRP's ectodomain from perivascular astrocytes under hypoxic

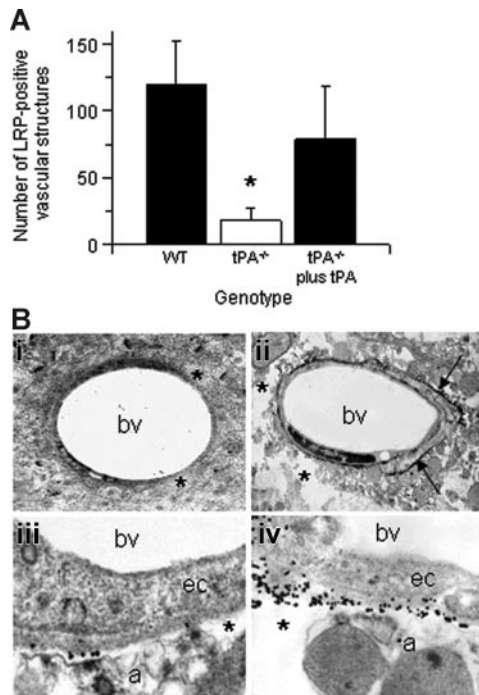


Figure 6. Effect of tPA on cerebral ischemia-induced shedding of LRP's ectodomain. (A) Number of LRP-positive vascular structures in wild-type (WT) and tPA^{-/-} mice in the 3 AOIs 24 hours after MCAO. A subset of tPA^{-/-} mice was intracerebrally injected with murine tPA immediately after MCAO (tPA^{-/-} plus tPA). Error bars describe standard error of the mean; n = 6; *P < .005 relative to WT and tPA^{-/-} plus tPA. (B) Electron microscopy analysis of LRP in the NVU in the area of developing cerebral edema 24 hours after MCAO in tPA^{-/-} mice intracerebrally injected with either PBS (i,iii) or recombinant tPA (ii,iv) immediately after MCAO. Brains were stained with the R2629 anti-LRP antibody. Arrows in panel Bii depict the presence of LRP around the blood vessel. Asterisks in panel Bii, iii, and iv denote areas of perivascular edema. A indicates astrocyte; bv, blood vessel; ec, endothelial cell. Magnification, $\times 5000$ (i-ii) and $\times 30\,000$ (iii-iv). Images were visualized using a Hitachi H-7500 electron microscope.

conditions, we subjected cultured astrocytes from wild-type and tPA^{-/-} mice to oxygen-glucose deprivation (OGD) conditions in serum-free media for 6 hours. Immunoblot analysis of cell extracts demonstrated that OGD increases the expression of cellular LRP in astrocytes from wild-type mice and that this effect is significantly decreased in astrocytes from tPA^{-/-} animals (Figure 7A-B). When the conditioned media was examined for shedding of the LRP ectodomain, we noted that exposure of wild-type astrocytes to OGD conditions resulted in a significant increase in the amount of LRP that was shed. However, this OGD-induced shedding of LRP was significantly decreased in astrocytes from tPA^{-/-} animals (Figure 7A). To further characterize the effect of tPA on the shedding of LRP's ectodomain we performed an immunoblot analysis of total cell extracts and conditioned medium from astrocytes cultured from wild-type mice and exposed to either normoxic or hypoxic conditions in the presence of exogenously added tPA. As a control, we also included RAP along with the tPA. Our results indicate that incubation with tPA results in a significant increase in OGD-induced shedding of LRP's ectodomain. This effect was inhibited in the absence of tPA and when the cultures were incubated with tPA and RAP simultaneously. Surprisingly, the effect of tPA on the shedding of LRP's ectodomain was also seen under normoxic conditions. Finally, the shedding of LRP was studied in astrocytes exposed to OGD conditions in the presence of RAP without tPA. Our data demonstrate that incubation with

RAP results in a significant decrease in OGD-induced shedding of LRP's ectodomain.

Discussion

The low-density lipoprotein receptor-related protein (LRP) is found in the human CNS in neurons and in perivascular astrocytic end-feet processes.³⁶ In neurons LRP has been found to mediate events such as long-term potentiation⁵ and calcium influx via NMDA receptors.³⁷ LRP is also expressed in smooth muscle cells (SMCs), and specific deletion of the LRP gene from vascular SMCs on a background of LDL-receptor deficiency causes SMC proliferation, increased susceptibility to cholesterol-induced atherosclerosis, and aneurysm formation.³⁸ The role of LRP in perivascular astrocytic end-feet processes is less well understood. However, the fact that almost 95% of the vascular basement membrane is embraced by astrocytic end-feet processes³⁹ suggests that LRP may play a role in the regulation of the function of this structure. The results of our immunohistochemical and electron microscopy studies indicate that cerebral ischemia induces shedding of LRP's ectodomain into the perivascular basement membrane in areas with evolving cerebral edema. Together, our data suggest a relation between shedding of LRP's ectodomain and increase in the permeability of the NVU.

The low permeability of the NVU is determined not only by an extremely low rate of transcytotic vesicles and a restrictive paracellular diffusion barrier through endothelial cells but also by the adhesion of astrocytes to the extracellular matrix.⁴⁰⁻⁴² Indeed, detachment of astrocytes from the extracellular matrix of the basal lamina results in edema and hemorrhage in the brain parenchyma.⁴⁰ The onset of the ischemic insult induces profound changes in the architecture of the NVU, including detachment of astrocytic end-feet processes from the basement membrane and degradation of components of the extracellular matrix,^{42,43} with resultant increase in the permeability of the BBB.⁴⁴ Our electron microscopy studies show that early after MCAO there is shedding of LRP's ectodomain into the basement membrane in areas of the NVU with astrocytic swelling and detachment of astrocytic end-feet processes from the basement membrane with formation of perivascular edema. On the basis of these observations we postulate that shedding of LRP may play a role in the development of the structural changes in the architecture of the NVU that result in an increase in the permeability of the BBB during cerebral ischemia.

The receptor-associated protein (RAP) is a receptor antagonist that prevents the interaction between LRP and its ligands.⁴⁵ The observation that antagonism of LRP with either RAP or anti-LRP antibodies results in inhibition of the shedding of LRP's ectodomain, preservation of the barrier function of the NVU, and a faster recovery of motor function following MCAO strongly supports the hypothesis that LRP plays a role in the maintenance of the permeability of the NVU. An alternative explanation to the observed decrease in the number of LRP-positive vascular structures in RAP-treated animals is that RAP could interfere with normal LRP immunodetection. This possibility is highly unlikely because RAP does not block the detection of LRP in enzyme-linked immunosorbent assay (ELISA) or immunoblotting experiments with the same antibody. Furthermore, we obtained similar results when animals were treated with anti-LRP antibodies.

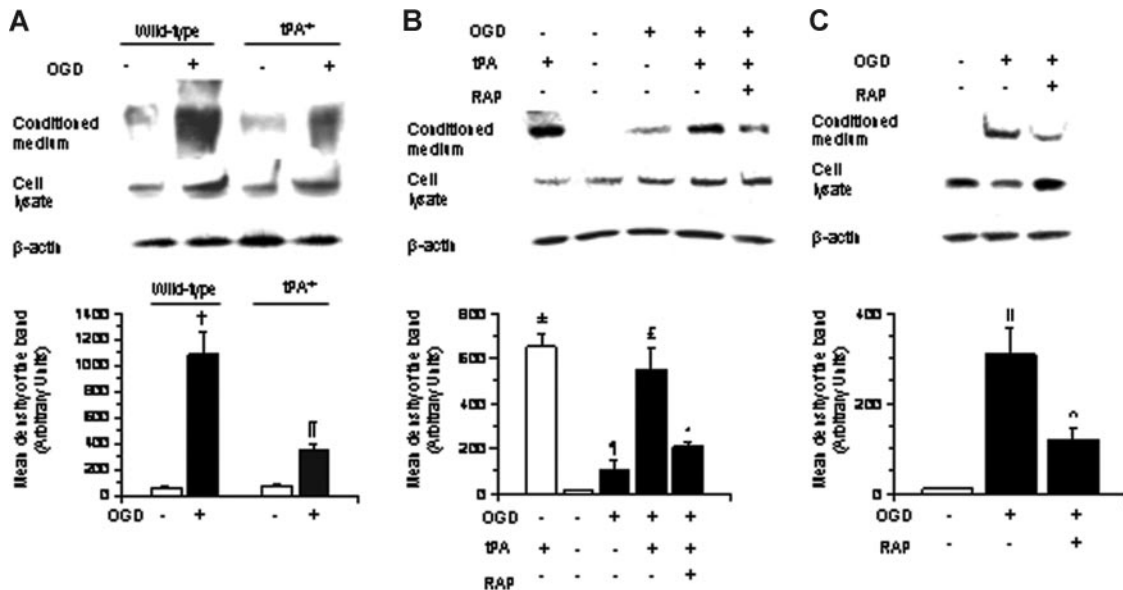


Figure 7. LRP shedding from murine astrocytes exposed to OGD conditions. (A) Representative immunoblot with the R2629 antibody of cell lysates and conditioned media of astrocytes from wild-type and tPA deficient (tPA^{-/-}) mice exposed to either normoxic or OGD conditions for 6 hours. Top panel shows LRP in the conditioned media, and lower panel represents LRP in cell lysates. Each observation was repeated 4 times. Bar graph describes mean density of the band per experimental group. Lines depict SEM. White bars represent results obtained under normoxic conditions. Black bars depict observations made under OGD conditions. † $P < .001$ and †† $P < .05$ relative to astrocytes exposed to normoxic conditions (B) Representative immunoblot with the R2629 antibody of cell lysates and conditioned medium of astrocytes from wild-type mice exposed to either normoxia or OGD conditions, in the presence or absence of either tPA or tPA and RAP. Upper panel shows LRP in the conditioned media and lower panel represents LRP in cell lysates. Each observation was repeated 4 times. Bar graph describes mean density of the band per experimental group. Lines depict SEM. White bars represent results obtained under normoxic conditions. Black bars depict observations made under OGD conditions. ± $P < .01$ and †† $P < .05$ relative to astrocytes exposed to normoxic conditions in absence of tPA. ‡ $P < .01$ relative to astrocytes exposed to OGD conditions without tPA or with tPA plus RAP. * $P < .05$ relative to astrocytes exposed to OGD conditions in the absence of tPA. (C) Representative immunoblot with the R2629 antibody of cell lysates and conditioned media of astrocytes from wild-type mice exposed to either normoxia or OGD conditions, in the presence or absence of RAP. Each observation was repeated 4 times. Bar graphs describe mean density of the band for a total of 4 observations per experimental group. Lines depict SEM. White bars represent results obtained under normoxic conditions. Black bars depict observations made under OGD conditions. ^ $P < .01$ relative to astrocytes maintained under normoxic conditions; †† $P < .05$ relative to astrocytes exposed to OGD conditions in the absence of RAP.

Tissue-type plasminogen activator is a serine proteinase that is found in both the intravascular space and in the CNS. In the intravascular space tPA's substrate is plasminogen,⁴⁶ and its main function is as a thrombolytic enzyme. Accordingly, based on its thrombolytic role, tPA is the only FDA-approved medication for the treatment of patients with acute ischemic stroke.⁴⁷ In contrast, the substrate of tPA in the CNS has not yet been well defined,^{48,49} and its presence in the brain has been linked not only with events associated with synaptic plasticity⁴⁹⁻⁵² but also with cell death,^{15,48} modulation of vascular tone,²⁵ and regulation of the permeability of the BBB under nonischemic conditions. Indeed, intraventricular administration of tPA results in an increase in the permeability of the BBB. The mechanism of this effect of tPA on the permeability of the NVU is unknown, but it is inhibited by treatment with either RAP or anti-LRP antibodies and is not observed when animals are treated with uPA instead of tPA.¹⁶

In vivo zymography assay studies have demonstrated that very early after the onset of the ischemic insult there is an increase in tPA activity in the NVU in the area surrounding the necrotic core.¹⁶ Our electron microscopy studies demonstrate that these are the same areas where we observe an early shedding of LRP's ectodomain around blood vessels with changes in the architecture of the NVU after MCAO. These findings and the fact that tPA is a ligand for LRP^{10,11} suggest that the interaction between tPA and LRP plays a role in the regulation of the permeability of the NVU during cerebral ischemia. This hypothesis is supported by our findings of a minimal shedding of LRP's ectodomain into the basement membrane of tPA^{-/-} mice after MCAO that increases

significantly when animals are treated with recombinant tPA immediately after the onset of the ischemic insult. The observation that either treatment with RAP or genetic deficiency of tPA protects the permeability of the NVU during cerebral ischemia and that treatment of tPA^{-/-} mice with murine tPA following the onset of the ischemic insult results in augmentation in Evans blue dye extravasation further support our hypothesis.

We postulate that in response to the ischemic insult there is shedding of LRP's ectodomain from the astrocytic end-feet processes into the basement membrane. This process is dependent on the presence of tPA and results in disruption of the structure of the NVU. A soluble form of LRP, shed from the cell surface, circulates in the plasma⁵³; thus, an alternative explanation to our findings is that the increase in LRP in the basement membrane during cerebral ischemia may be the result of the passage of plasma components across an already abnormally permeable BBB and not the result of shedding of LRP from perivascular astrocytes. This possibility seems unlikely for 2 main reasons. First, immunohistochemical and electron microscopy studies indicate a total absence of LRP in endothelial cells and interendothelial tight junctions which we would expect to be heavily stained if soluble LRP originated from the circulation. Second, our in vitro experiments indicate that tPA induces shedding of the LRP's ectodomain from astrocytes cultured in serum-free media.

Moreover, the demonstration that OGD induces shedding of LRP from wild-type astrocytes and that this shedding is significantly decreased in astrocytes from tPA^{-/-} mice suggests that the interaction between tPA and LRP under ischemic conditions takes

place in the abluminal side of the NVU, in the interface between astrocytic end-feet processes, and the basement membrane. Surprisingly, we found that tPA also induces shedding of LRP's ectodomain from cultured astrocytes under nonischemic conditions. This observation suggests that tPA is necessary and sufficient to induce shedding of LRP's ectodomain and that this process results in disruption of the integrity of the NVU. Recent studies have demonstrated that tPA can cross the intact BBB by LRP-mediated transcytosis⁵⁴ and that this process is exacerbated by exposure to OGD.⁵⁵ Thus, it is possible that in the earlier phases of cerebral ischemia the cleavage of LRP's ectodomain is the result of the effect of astrocyte-derived tPA and that this process is enhanced in later phases by the passage of intravascular tPA into the ischemic tissue.

On the basis of our results we propose a model where in response to the ischemic insult there is an increase in tPA activity around the NVU. The interaction between this tPA and LRP in astrocytic end-feet processes results in cleavage of LRP's ectodomain which is shed into the basement membrane. This results in release of the intracellular tail of LRP into the cytoplasm which may activate signaling pathways with resultant detachment of astrocytic end-feet processes from the glia limitans and increase in the permeability of the NVU.

References

- Herz J, Strickland DK. LRP: a multifunctional scavenger and signaling receptor. *J Clin Invest.* 2001;108:779-784.
- Kowal RC, Herz J, Goldstein JL, Esser V, Brown MS. Low density lipoprotein receptor-related protein mediates uptake of cholesteryl esters derived from apoprotein E-enriched lipoproteins. *Proc Natl Acad Sci U S A.* 1989;86:5810-5814.
- Strickland DK, Ashcom JD, Williams S, et al. Sequence identity between the alpha 2-macroglobulin receptor and low density lipoprotein receptor-related protein suggests that this molecule is a multifunctional receptor. *J Biol Chem.* 1990;265:17401-17404.
- Herz J. The LDL receptor gene family: (un)expected signal transducers in the brain. *Neuron.* 2001;29:571-581.
- Zhuo M, Holtzman DM, Li Y, et al. Role of tissue plasminogen activator receptor LRP in hippocampal long-term potentiation. *J Neurosci.* 2000;20:542-549.
- Blaumueller CM, Qi H, Zagouras P, Artavanis-Tsakonas S. Intracellular cleavage of Notch leads to a heterodimeric receptor on the plasma membrane. *Cell.* 1997;90:281-291.
- Cao X, Sudhof TC. A transcriptionally [correction of transcriptionally] active complex of APP with Fe65 and histone acetyltransferase Tip60. *Science.* 2001;293:115-120.
- May P, Reddy YK, Herz J. Proteolytic processing of low density lipoprotein receptor-related protein mediates regulated release of its intracellular domain. *J Biol Chem.* 2002;277:18736-18743.
- Quinn KA, Pye VJ, Dai YP, Chesterman CN, Owensby DA. Characterization of the soluble form of the low density lipoprotein receptor-related protein (LRP). *Exp Cell Res.* 1999;251:433-441.
- Bu G, Morton PA, Schwartz AL. Identification and partial characterization by chemical cross-linking of a binding protein for tissue-type plasminogen activator (t-PA) on rat hepatoma cells. A plasminogen activator inhibitor type 1-independent t-PA receptor. *J Biol Chem.* 1992;267:15595-15602.
- Bu G, Williams S, Strickland DK, Schwartz AL. Low density lipoprotein receptor-related protein/alpha 2-macroglobulin receptor is a hepatic receptor for tissue-type plasminogen activator. *Proc Natl Acad Sci U S A.* 1992;89:7427-7431.
- Hu K, Yang J, Tanaka S, et al. Tissue-type plasminogen activator acts as a cytokine that triggers intracellular signal transduction and induces matrix metalloproteinase-9 gene expression. *J Biol Chem.* 2006;281:2120-2127.
- Wang X, Lee SR, Arai K, et al. Lipoprotein receptor-mediated induction of matrix metalloproteinase by tissue plasminogen activator. *Nat Med.* 2003;10:1313-1317.
- Wang YF, Tsirka SE, Strickland S, et al. Tissue plasminogen activator (tPA) increases neuronal damage after focal cerebral ischemia in wild-type and tPA-deficient mice. *Nat Med.* 1998;4:228-231.
- Yepes M, Sandkvist M, Wong MK, et al. Neuroserpin reduces cerebral infarct volume and protects neurons from ischemia-induced apoptosis. *Blood.* 2000;96:569-576.
- Yepes M, Sandkvist M, Moore EG, et al. Tissue-type plasminogen activator induces opening of the blood-brain barrier via the LDL receptor-related protein. *J Clin Invest.* 2003;112:1533-1540.
- Nagai N, De Mol M, Lijnen HR, Carmeliet P, Colten D. Role of plasminogen system components in focal cerebral ischemic infarction: a gene targeting and gene transfer study in mice. *Circulation.* 1999;99:2440-2444.
- Cinelli P, Madani R, Tsuzuki N, et al. Neuroserpin, a neuroprotective factor in focal ischemic stroke. *Mol Cell Neurosci.* 2001;18:443-457.
- del Zoppo GJ, Mabuchi T. Cerebral microvessel responses to focal ischemia. *J Cereb Blood Flow Metab.* 2003;23:879-894.
- Lo EH, Dalkara T, Moskowitz MA. Mechanisms, challenges and opportunities in stroke. *Nat Rev Neurosci.* 2003;4:399-415.
- Rubin LL, Staddon JM. The cell biology of the blood-brain barrier. *Annu Rev Neurosci.* 1999;22:11-28.
- Wolburg H, Lippoldt A. Tight junctions of the blood-brain barrier: development, composition and regulation. *Vascul Pharmacol.* 2002;38:323-337.
- Baker RN, Cancilla PA, Pollock PS, Frommes SP. The movement of exogenous protein in experimental cerebral edema. An electron microscopic study after freeze-injury. *J Neuropathol Exp Neurol.* 1971;30:668-679.
- Garcia JH, Lossinsky AS, Kauffman FC, Conger KA. Neuronal ischemic injury: light microscopy, ultrastructure and biochemistry. *Acta Neuropathol (Berl).* 1978;43:85-95.
- Nassar T, Akkawi S, Shina A, et al. The in vitro and in vivo effect of tPA and PAI-1 on blood vessel tone. *Blood.* 2004;103:897-902.
- Herz J, Kowal RC, Ho YK, Brown MS, Goldstein JL. Low density lipoprotein receptor-related protein mediates endocytosis of monoclonal antibodies in cultured cells and rabbit liver. *J Biol Chem.* 1990;265:21355-21362.
- Newton CS, Loukinova E, Mikhailenko I, et al. Platelet-derived growth factor receptor-beta (PDGFR-beta) activation promotes its association with the LDL receptor-related protein (LRP): evidence for co-receptor function. *J Biol Chem.* 2005;280:27872-27878.
- Ranganathan S, Liu CX, Migliorini MM, et al. Serine and threonine phosphorylation of the low density lipoprotein receptor-related protein by protein kinase Calpha regulates endocytosis and association with adaptor molecules. *J Biol Chem.* 2004;279:40536-40544.
- Paxinos G, Franklin KBJ. *The Mouse Brain in Stereotaxic Coordinates.* San Diego, CA: Academic Press Inc; 2001.
- Meyding-Lamade U, Ehrhart K, de Ruiz HL, Kehm R, Lamade W. A new technique: serial puncture of the cisterna magna for obtaining cerebrospinal fluid in the mouse—application in a model of herpes simplex virus encephalitis. *J Exp Anim Sci.* 1996;38:77-81.
- Tamura A, Graham DI, McCulloch J, Teasdale GM. Focal cerebral ischaemia in the rat, 1: description of technique and early neuropathological consequences following middle cerebral artery occlusion. *J Cereb Blood Flow Metab.* 1981;1:53-60.
- Polavarapu R, Gongora MC, Winkles JA, Yepes M. Tumor necrosis factor-like weak inducer of

Acknowledgment

We thank Mr Qiang Shen from the Yerkes National Primate Research Center at Emory University for his assistance with the magnetic resonance imaging studies.

This work was supported by the National Institutes of Health (grant NS49478) (M.Y.), (grants HL50784 and HL54710) (D.S.), and (grants HL055374 and HL055747) (D.A.L.).

Authorship

Contribution: R.P., M.C.G., H.Y. and S.R. performed the research; D.A.L. designed the research; D.S. designed the research and contributed vital reagents; M.Y. designed and performed the research and wrote the paper.

Conflict-of-interest disclosure: The authors declare no competing financial interests.

Correspondence: Manuel Yepes, Department of Neurology and Center for Neurodegenerative Disease, Whitehead Biomedical Research Bldg, 615 Michael St, Ste 505J, Atlanta, GA 30322; e-mail address: myepes@emory.edu.

- apoptosis increases the permeability of the neurovascular unit through nuclear factor-kappaB pathway activation. *J Neurosci*. 2005;25:10094-10100.
33. Zhang X, Winkles JA, Gongora MC, et al. TWEAK-Fn14 pathway inhibition protects the integrity of the neurovascular unit during cerebral ischemia. *J Cereb Blood Flow Metab*. Prepublished on July 12, 2006, as DOI 10.1038/sj.jcbfm.9600368.
 34. Yepes M, Moore E, Brown SA, et al. Progressive ankylosis (Ank) protein is expressed by neurons and Ank immunohistochemical reactivity is increased by limbic seizures. *Lab Invest* 2003;83:1025-1032.
 35. Berry I, Ranjeva JP, Duthil P, Manelfe C. Diffusion and perfusion MRI, measurements of acute stroke events and outcome: present practice and future hope. *Cerebrovasc Dis*. 1998;8(suppl 2):8-16.
 36. Wolf BB, Lopes MB, VandenBerg SR, Gonias SL. Characterization and immunohistochemical localization of alpha 2-macroglobulin receptor (low-density lipoprotein receptor-related protein) in human brain. *Am J Pathol*. 1992;141:37-42.
 37. Bacskai BJ, Xia MQ, Strickland DK, Rebeck GW, Hyman BT. The endocytic receptor protein LRP also mediates neuronal calcium signaling via N-methyl-D-aspartate receptors. *Proc Natl Acad Sci U S A*. 2000;97:11551-11556.
 38. Boucher P, Gotthardt M, Li WP, Anderson RG, Herz J. LRP: role in vascular wall integrity and protection from atherosclerosis. *Science* 2003;300:329-332.
 39. Vorbodt AW, Dobrogowska DH. Molecular anatomy of intercellular junctions in brain endothelial and epithelial barriers: electron microscopist's view. *Brain Res Brain Res Rev*. 2003;42:221-242.
 40. Risau W, Wolburg H. Development of the blood-brain barrier. *Trends Neurosci*. 1990;13:174-178.
 41. Wolburg H, Neuhaus J, Kniesel U, et al. Modulation of tight junction structure in blood-brain barrier endothelial cells. Effects of tissue culture, second messengers and cocultured astrocytes. *J Cell Sci*. 1994;107:1347-1357.
 42. Hamann GF, Okada Y, Fritridge R, del Zoppo GJ. Microvascular basal lamina antigens disappear during cerebral ischemia and reperfusion. *Stroke*. 1995;26:2120-2126.
 43. Hamann GF, Okada Y, del Zoppo GJ. Hemorrhagic transformation and microvascular integrity during focal cerebral ischemia/reperfusion. *J Cereb Blood Flow Metab*. 1996;16:1373-1378.
 44. Gotoh O, Asano T, Koide T, Takakura K. Ischemic brain edema following occlusion of the middle cerebral artery in the rat. I: the time courses of the brain water, sodium and potassium contents and blood-brain barrier permeability to 125I-albumin. *Stroke*. 1985;16:101-109.
 45. Williams SE, Ashcom JD, Argraves WS, Strickland DK. A novel mechanism for controlling the activity of alpha 2-macroglobulin receptor/low density lipoprotein receptor-related protein. Multiple regulatory sites for 39-kDa receptor-associated protein. *J Biol Chem*. 1992;267:9035-9040.
 46. Bugge TH, Kombrinck KW, Flick MJ, et al. Loss of fibrinogen rescues mice from the pleiotropic effects of plasminogen deficiency. *Cell*. 1996;87:709-719.
 47. The National Institute of Neurological Disorders and Stroke rt-PA Stroke Study Group. Tissue plasminogen activator for acute ischemic stroke. *N Engl J Med*. 1995;333:1581-1587.
 48. Tsirka SE, Gualandris A, Amaral DG, Strickland S. Excitotoxin-induced neuronal degeneration and seizure are mediated by tissue plasminogen activator. *Nature*. 1995;377:340-344.
 49. Yepes M, Sandkvist M, Coleman TA, et al. Regulation of seizure spreading by neuroserpin and tissue-type plasminogen activator is plasminogen-independent. *J Clin Invest*. 2002;109:1571-1578.
 50. Qian Z, Gilbert ME, Colicos MA, Kandel ER, Kuhl D. Tissue-plasminogen activator is induced as an immediate-early gene during seizure, kindling and long-term potentiation. *Nature*. 1993;361:453-457.
 51. Seeds NW, Williams BL, Bickford PC. Tissue plasminogen activator induction in Purkinje neurons after cerebellar motor learning. *Science*. 1995;270:1992-1994.
 52. Mataga N, Nagai N, Hensch TK. Permissive proteolytic activity for visual cortical plasticity. *Proc Natl Acad Sci U S A*. 2002;99:7717-7721.
 53. Quinn KA, Grimsley PG, Dai YP, et al. Soluble low density lipoprotein receptor-related protein (LRP) circulates in human plasma. *J Biol Chem*. 1997;272:23946-23951.
 54. Benchenane K, Berezowski V, Ali C, et al. Tissue-type plasminogen activator crosses the intact blood-brain barrier by low-density lipoprotein receptor-related protein-mediated transcytosis. *Circulation*. 2005;111:2241-2249.
 55. Benchenane K, Berezowski V, Fernandez-Monreal M, et al. Oxygen glucose deprivation switches the transport of tPA across the blood-brain barrier from an LRP-dependent to an increased LRP-independent process. *Stroke*. 2005;36:1065-1070.